Biointerface Research in Applied Chemistry
Platinum Open Access Journal (ISSN: 2069-5837)

Article
Volume 11, Issue 3, 2021, 10016 - 10026
https://doi.org/10.33263/BRIAC113.1001610026

Variety of Spike Protein in COVID-19 Mutation: Stability, Effectiveness and Outbreak Rate as a Target for Vaccine and Therapeutic Development

Majid Monajjemi [*,1], Fatemeh Mollaamin [1], Azadeh Sadat Shekarabi [1], Azam Ghadami [1]

[1] Department of Chemical Engineering, Central Tehran Branch, Islamic Azad University, Tehran, Iran
* Correspondence: maj.monajjemi@iauctb.ac.ir;

Scopus Author ID 6701810683
Received: 4.08.2020; Revised: 18.09.2020; Accepted: 21.09.2020; Published: 24.09.2020

Abstract: The structure of β-coronavirus MERS-CoV S1-CTD demonstrated an interesting subject of how two structurally similar viral RBDs recognize different protein receptors. Same as SARS-CoV, the S1-CTD, MERS-CoV S1-CTD viruses also contains two subdomains, but, in contrast to the loop-dominated MERS-CoV, RBM contains a 4-stranded antiparallel β-sheet, showing a relatively flat surface to bind DPP4. The protein sequences were obtained from NCBI web sites, and the proteins of COVID-19, such as protein sequences, were applied for analyzing the conserved domain. Some proteins were also utilized for constructing 3-D structures via homology modeling. We also show that N-terminal deletions of alpha 2 that no longer block STAT1 nuclear import. Covid-19 spike protein structures, along with peptide-like inhibitor structure of the SARS-CoV-2 spike glycoprotein, including small-molecule inhibitors, have been simulated via Molecular dynamic and docking methods. Several genomes of various coronaviruses using BAST and MAFFT software have been evaluated, and a few genomes have been selected.

Keywords: mutations; COVID-19; MERS-CoV RBM; spike protein.

1. Introduction

One of the important part of SARS-CoV-2, as well as several other COVID viruses, are the presence of spike proteins which allow these viruses for penetrating host cells and consequently cause infection (figure 1). The S-proteins are trans-membrane proteins glycosylated, which are made up of 1200 to 1500 amino acids, based on a variety of viruses [1]. S proteins are major components in SARS CoV2, where play an essential role in cell entry, approximately 1300aa long proteins, including two main sub-domains, which are structured as S_1 and S_2 In COVID-19, that is a beta-coronavirus from bat coronaviruses and infects humans. Structural details demonstrated that COVID-19 extracted from a bat SARS-like coronavirus and has mutated in the S-protein & N-proteins [2]. The COVID-19 complete genomes to possess fourteen open reading frames (ORFs) encoding 28 proteins. Sequences analyzing exhibited that COVID-19 has more than 85% identity with SARS-CoV and 55% with MERS-CoV. S_1 receptor binding domain or RBD and mediates viruses attachment to their ACE2 receptors, while S_2 carries out the function of fusion to enable successful entry [3]. S_2 contains the fusion peptide. As compared to the E &M proteins in virus assembling, the S proteins have a major role in the host cells and initiating infection [4]. As mentioned above S proteins could be divided into two important functional subunits, which include the N-terminal

S_1 and the C-terminal S_2 region. The S1 subunit can be attached to the receptors on the host cell, whilst the S_2 will be responsible for fusing the envelope of the virus is related to cell membranes [5]. In the ORFs group, the ORF1a/b can translate two polypeptides with the names, pp1(a) and pp1(ab), and also encodes 15 non-structural proteins. The residual ORFs encode other structural polypeptides, including spike(S), (E), (M), and nucleon-capsid (N) [6]. COVID-19 also possesses secondary proteins that participate with the host's innate immune response. S-proteins are the same as a molecular machine where mediates coronavirus entry into host cells and also binds to the receptors through its S_1 domains and then fuses viral through its S_2 component [6]. Spike protein consists of 3 parts: including a large Ecto-domain, a single-pass Tran's membrane anchor, and a short intracellular tail (scheme 1) [3-6]. Electron microscopy investigation showed where the spike proteins have a clove-shaped timer form with three S_1 heads and a trimmer's form of S_2 stalk. As soon as virus entry inside the cell, S_1 binds to the related receptor for viral binding, and S_2 also fuses the cell and viral membranes. Receptor binding is the critical situation in the beginning process of the coronavirus infection life [7,8].

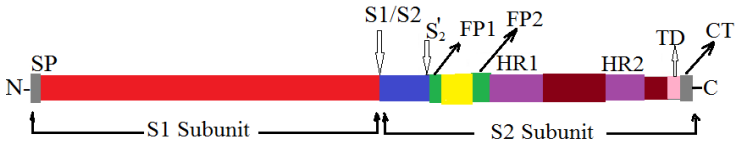

Scheme 1. Schematic position of two proteolytic cleavage sites (S1/S2 and S'$_2$), two proposed fusion peptides (FP1 and FP2), two heptad repeat regions (HR1 and HR2), transmembrane domain (TD), and cytoplasmic tail (CT).

1.1. How S protein allows coronaviruses to enter cells.

Right away, the S_1 attaches to the receptors, two major changing of systems can occur for the S_2 subunit to complete the fusion of the virus. Those are consisting of heptad repeat (HR) regions 1 and two, otherwise referred to as HR_1 and HR_2 (Scheme 1). The first confirmation is related to the transformation of an un-structured S_2 subunit and, in addition, the second conformational change for occurring, including the inversion of these subunits to the coils. As soon as these shapes are completed, the fusion peptide bonds are anchored to the cell of the host for allowing the virus to move towards the membranes [9,10].

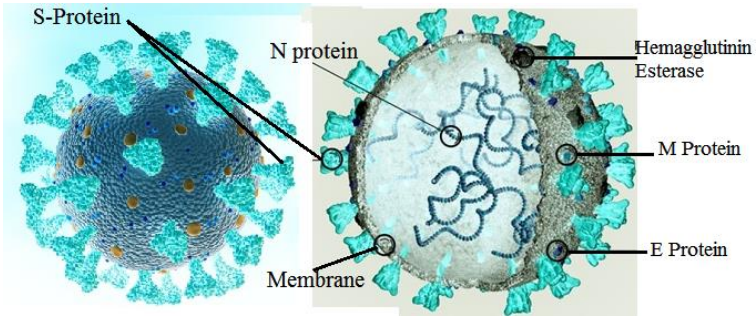

Figure 1. Component of COVID-19.

1.2. Receptor recognition.

The β-coronavirus SARS-CoV S1-CTD combined with human's ACE2 includes; two subunits, one a core structure and second a receptor-binding motif or RBM. The RBM demonstrated gradually concave outer surfaces for attaching ACE_2. The base of these concave surfaces are small, two-stranded antiparallel β-sheets, and two ridges are completed through several loops. Several virus-binding motifs (VBMs) have been identified on the outer surfaces

of the peptidase, away from the buried peptidase catalytic ports. Studies on CoV-ACE2 combinations have been prepared some new concepts inside cross-species transmissions. Within this epidemic, similar SARS-CoV was abstracted from both human patients. Between both of the themes a salt bridge, including a hydrophobic media, appears to the virus-receptor binding. Two residues in beta-CoV S_1-CTD complexes are under mutation, and these played major roles in the civet-to-human and human-to-human transmissions during the epidemic.

The shape of β-coronavirus MERS-CoV S1-CTD demonstrated an important example of how two structurally viral RBDs recognize various protein receptors. Same as SARS-CoV S1-CTD, MERS-CoV S1-CTD also contains two subdomains, but, in contrast to the loop-dominated MERS-CoV, RBM contains a four-stranded antiparallel β-sheet, presenting a relatively flat surface to bind DPP4. Various MERS-of coronaviruses family have been isolated from bats (Figure 2) [11-14].

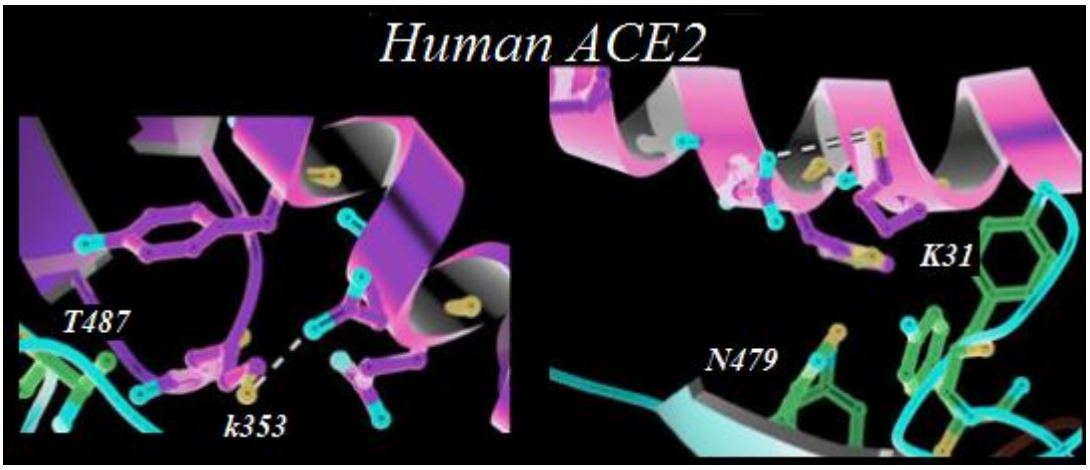

Figure 2. Human Sars-Cov S1-CTD.

1.3. Targeting viruses via the S protein.

By the lake of S-protein, COVID-19 would never be able to react with the cell of humans to cause infection. Consequently, S-proteins exhibit a suitable target for vaccines. Moreover, in cells, S protein of viruses is a major inducer of antibodies that naturally produced through our human immune systems. So, this kind of antibody binds to the surface of a viral system to prevent their entry into human cells, and some of them have been recognized against SARS -CoV containing domain targets.

The most sensitivities of the S-subunits have led other scientists to be attempted in researching standardized agents that can stop the binding activities and fusion of S-proteins in SARS-CoV-2. Although recent works have discovered that the neutralization capabilities of those drugs against the SARS-CoV-2 within the S1 subunits are uncertain, some studies have exhibited that drug has a stronger neutralization capability as compared to when these are given alone. This information, therefore, leads scientists to believe that a combination of several potent drugs has the potential to target SARS-CoV-2 and increase its sensitivity to neutralization [12-15].

1.4. Fusion mechanism.

Spike proteins are important for any further studies, so during molecular maturation, it is cleaved via host proteases into receptor-attaching subunit HA_1 and membrane-fusion subunit

HA_2. During cell entry, HA_1 appends to the sugar receptors of viral structures, and after that HA_1 dissociates, and then HA_2 changes towards the transition of the post-fusion positions. Consequently, the buried hydrophobic fusion peptides in HA_2 become exposed and insert into the target host membrane (Figure 3).

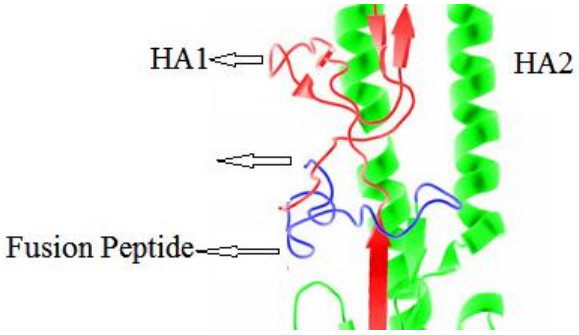

Figure 3. Hemagglutinin glycoprotein (HA) into receptor-binding subunit HA_1 and membrane-fusion subunit HA_2.

The fusion peptide is eventually positioned on the same end of the six-helical structures, yield the viral and host membranes together to fuse. Due to six-helical structures that are energetically stables, huge amounts of energies are released during the conformational transition of HA. These structures of the perfusion COVID- spike proteins are also more complex than that of influenza virus HA. In spike structures, S_1 heads (on top of an S_2) preventing S_2 from undergoing conformational transitions. In addition, in the S_2 stalk, HR-N forms several helical conformations and arranges by themselves along the symmetry axis of S_2 subunits.

2. Materials and Methods

All computational calculations were done using the Gaussian, Hyper Chem, Chem office, Charmm, and Schrodinger packages. Covid-19 spike structures, along with peptides like inhibitors molecules of the SARS-CoV-2 spike glycoprotein (PDB ID: 6VXX, DOI:10.2210/pdb6VXX/pdb) including small-molecules of inhibitor structures (Figure 4) and model of novel coronavirus spike-receptor-binding domain complexes with its receptors ACE2 (Pdb ID:6LZG DOI:10.2210/pdb6LZG/pdb) (PDB ID: 6W63) (Figure 5), were designed and simulated from related PDB of SARS-Cov-2 main protease. The majorities of those structures are bind with small molecules and are suitable for the drug discovery approaches. Proteins were provided in protein preparation wizard, H atoms have been added, and H_2O molecules beyond 6Å of the binding sites were removed. The chains and loops were designed using the prime module.

2.1. Docking and free energy calculations.

BIOVIA-2020's Docking software, chem3D, Hyper Chem, Rasmol, VMD, and Charmm software have been applied for all optimization and docking calculation. The grids of 20& 19Å were produced over the co-crystallized peptide-like inhibitors. Re-docking of the co-crystallized molecules was accomplished for evaluating the docking protocols. The docked systems were based on crystal structures for calculating the root mean square deviation. The re-docking of structures and compounds pose with 1.20Å and 0.70Å RMSD, respectively. Lower RMSD demonstrates that our docking methodologies are adequate and can be applied to search small molecule inhibitors. Docking was done in 3 different modes, virtual screening

followed by standard-precision (SP) and extra-precision (XP) docking using the Glide program.

2.2. M.D. simulations.

Molecular dynamics modeling for polypeptide-ligands structures were accomplished using the above-mentioned software. The OPLS and Charmm force fields were applied for modeling the interactions of the protein-small molecules. Long-range electrostatic forces were estimated using the Particle-mesh E-wald (PME) software with a grid spacing of 0.75 Å. Nose-Hoover thermometry and Martyna-Tobias-Klein method were applied for maintaining the temperature and constant pressure, respectively. The formula of motion was considered using the multi-run RESPA by 3.0 fs time steps for bonded and non-bonded interactions within a low cutoff. An outer time step of 5.0 fs was used for non-bonded forces beyond the cutoff.

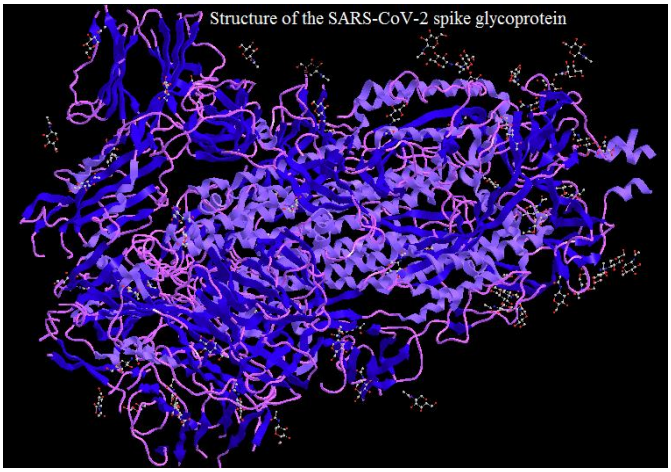

Figure 4. Structure, function, and antigenicity of the SARS-CoV-2 spike glycoprotein.

2.3. Simulations for interactions between the CoV2-RBD and the ACE2.

It can be discussed widely about the charged residues for many of the fraction and binding interface of CoV2-RBD and the ACE2. Moreover, electrostatic interactions have critical points for a complex formation. Distances among the two mentioned proteins are a key at the binding interfaces that identified for the three representative models (Figure 5 & Table 1).

Table 1. Human-derived anti-SARS-CoV-2 S protein RBD neutralizing antibody and nucleocapsid antibody (Contact residues).

Molecule	Cat. No.	Species	Host	Product Description
Nucleocapsid protein	AC2-H5257	Human	HEK293	Human ACE2 / ACEH Protein, Fc Tag (MALS verified)
	AC2-C52H7	Cynomolgus	HEK293	Cynomolgus ACE2 / ACEH Protein, His Tag
	AC2-H52H8	Human	HEK293	Human ACE2 / ACEH Protein, His Tag (MALS verified)
	AC2-R5246	Rat	HEK293	Rat ACE2 / ACEH Protein, His Tag (MALS verified)
	AC2-M5248	Mouse	HEK293	Mouse ACE2 / ACEH Protein, His Tag (MALS verified)
	AC2-P5248	Paguma larvata	HEK293	Paguma larvata ACE2 / ACEH Protein, His Tag
	NUN-V52H3	HCoV-OC43	HEK293	HCoV-OC43 Nucleocapsid protein, His Tag
S1 protein	S1N-C52H3	SARS-CoV-2	HEK293	SARS-CoV-2 (COVID-19) S1 protein, His Tag
	S1N-S52H5	SARS	HEK293	SARS S1 protein, His Tag (MALS verified)
	S1N-C52H4	SARS-CoV-2	HEK293	SARS-CoV-2 (COVID-19) S1 protein, His Tag (MALS verified)
	S1N-C5255	SARS-CoV-2	HEK293	SARS-CoV-2 (COVID-19) S1 protein, Fc Tag
	S1N-C5257	SARS-CoV-2	HEK293	SARS-CoV-2 (COVID-19) S1 protein, Mouse IgG2a Fc Tag
S2 protein	S2N-C52H5	SARS-CoV-2	HEK293	SARS-CoV-2 (COVID-19) S2 protein, His Tag
S protein RBD	SPD-C5255	SARS-CoV-2	HEK293	SARS-CoV-2 (COVID-19) S protein RBD, Fc Tag (MALS verified)

Molecule	Cat. No.	Species	Host	Product Description
	SPD-S52H6	SARS	HEK293	SARS S protein RBD, His Tag (MALS verified)
	SPD-C5259	SARS-CoV-2	HEK293	SARS-CoV-2 (COVID-19) S protein RBD, Mouse IgG2a Fc Tag
	SPD-S52H5	SARS-CoV-2	HEK293	SARS-CoV-2 (COVID-19) S protein RBD (N354D), His Tag
	SPD-S52H7	SARS-CoV-2	HEK293	SARS-CoV-2 (COVID-19) S protein RBD (W436R), His Tag
	SPD-S52H8	SARS-CoV-2	HEK293	SARS-CoV-2 (COVID-19) S protein RBD (R408I), His Tag
	SPD-C52H4	SARS-CoV-2	HEK293	SARS-CoV-2 (COVID-19) S protein RBD (G476S), His Tag
S1 protein CTD	S1D-C52H3	SARS-CoV-2	HEK293	SARS-CoV-2 (COVID-19) S1 protein CTD, His Tag
S protein	SPN-C52H4	SARS-CoV-2	HEK293	SARS-CoV-2 (COVID-19) S protein (R683A, R685A), His Tag
	SPN-C52H8	SARS-CoV-2	HEK293	SARS-CoV-2 (COVID-19) S protein (R683A, R685A) , His Tag, active trimer (MALS verified)
Envelope protein	ENN-C5128	SARS-CoV-2	*E.coli*	SARS-CoV-2 (COVID-19) Envelope protein, His Tag
Papain-like Protease	PAE-C5148	SARS-CoV-2	*E.coli*	SARS-CoV-2 (COVID-19) Papain-like Protease Protein, His Tag
Nucleocapsid protein	NUN-C51H9	SARS-CoV-2	*E.coli*	SARS-CoV-2 (COVID-19) Nucleocapsid protein, His Tag
	NUN-C5227	SARS-CoV-2	HEK293	SARS-CoV-2 (COVID-19) Nucleocapsid protein, His Tag
	NUN-C81Q6	SARS-CoV-2	*E.coli*	Biotinylated SARS-CoV-2 (COVID-19) Nucleocapsid protein, His, Avitag™
S1 protein	SIN-V52H3	HCoV-NL63	HEK293	HCoV-NL63 S1 protein, His Tag
	SIN-V52H4	HCoV-229E	HEK293	HCoV-229E S1 protein, His Tag
	SIN-V52H5	HCoV-OC43	HEK293	HCoV-OC43 S1 protein, His Tag
	SIN-V52H6	HCoV-HKU1(isolate N5)	HEK293	HCoV-HKU1(isolate N5) S1 protein, His Tag
NSP1	NS1-C51H7	SARS-CoV-2	*E.coli*	SARS-CoV-2 (COVID-19) NSP1 Protein, His Tag
NSP7	NS7-C51H6	SARS-CoV-2	*E.coli*	SARS-CoV-2 (COVID-19) NSP7 Protein, His Tag

The majority of those residues are preserved for our simulation. The same models can be accomplished for the SARS-RBD/ACE2 complexes. Interestingly, the SARS-RBD match in CoV2-RBD did not form close with the ACE2 in related simulations. It is worthwhile to mention that the sequence identity between CoV2-RBD and SARS-RBD is low in this loop region, suggesting the loop region might be partially responsible for the difference in the receptor binding. The H-bonds among the CoV2-RBD and ACE2 can be extracted using the VMD program. It can be discussed that the number of hydrogen bonds fluctuated over time. Similar trends can be observed in the other simulations, suggesting that the binding became stronger as the simulation progressed. This work has been done based on our theoretical works [17-75].

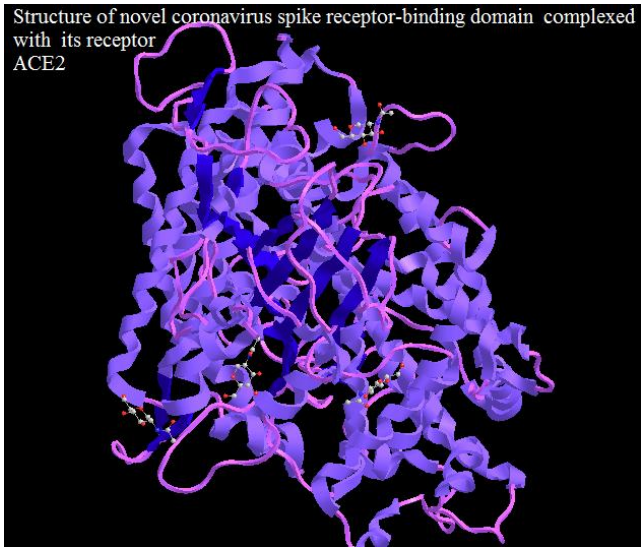

Figure 5. Structure of novel coronavirus spike receptor-binding domain complexed with its receptor ACE2.

3. Results and Discussion

An active inhibitor of HIV-1 protease was found effective in treating COVID-19 disease. Data from the docking calculations were analyzed by the molecular modeling software [76,77]. We accomplished 60 ns molecular dynamic modeling (MD) of both SARS-CoV and COVID-19 to get insight into the binding cavities with a classical molecular dynamics method with water molecules applied as molecular indexes. These kinds of strategies are supposed to provide highly detailed pictures of protein's interior dynamics. These small molecules tracking approaches were applied for determining the accessibilities of the pockets of the active sites in both SARS-CoV and COVID-19, and also, the local distribution approaches were applied for providing information about an overall distribution of related solvents in the protein interior. To properly examine the flexibilities of both activated sites, we applied the AQUA-DUCT (AQ) software for analyzing the water molecules flow through the cavities in a 15 ns time step. Effectiveness and Outbreak rate as a target for vaccine and therapeutic development has been an important factor for anti-HCoVs drugs. RBD of the S protein has been proposed as a promising target for the development of specific antibodies and vaccines. RBD-specific antibody CDC2-C2 demonstrated inhibitory activities against MERS-CoV infection. CoV-S-RBD is hyper-variable throughout evolution, which marking differences in host receptors usage in different H-CoVs. Although the same host receptors are used by different H-CoVs, they frequently target different binding sites on the host receptor. For this reason, specific RBD-active sites, antibodies or vaccines inevitably lack broad-spectrum activities against coronavirus infection. The delay time among emerging human CoVid-19 outbreaks and the development of new prophylactic treatments or vaccines are of concern.

4. Conclusions

Thus, there is an urgent need for the development of new, broad-spectrum drugs that target conserved sites in the currently circulating and future emerging coronavirus so as to prepare for future outbreaks of yet unknown COVID-19 added to the manuscript even if the discussion is unusually long or complex.

Funding

This research was funded by ourselves.

Acknowledgments

Thanks to the Central Tehran Branch, Islamic Azad University for supporting computational software and all necessary equipment.

Conflicts of Interest

The authors declare no conflict of interest.

References

1. Lana, R.M.; Coelho, F.C.; Gomes, M.F.d.C.; Cruz, O.G.; Bastos, L.S.; Villela, D.A.M.; Codeço, C.T. The novel coronavirus (SARS-CoV-2) emergency and the role of timely and effective national health surveillance. *Rep Public Health* **2020**, http://doi.org/10.1590/0102-311X00019620.
2. Baglivo, M.; Baronio, M.; Natalini, G.; Beccari, T.; Chiurazzi, P.; Fulcheri, E.; Petralia, P.; Michelini, S.; Fiorentini, G.; Miggiano, G.; Morresi, A.; Tonini, G.; Bertelli, M. Natural small molecules as inhibitors of

coronavirus lipiddependent attachment to host cells a possible strategy for reducing SARS-COV-2 infectivity? *Acta Biomed* **2020**, *91*, 161–4, https://doi.org/10.23750/abm.v91i1.9402.
3. Thomso, G. COVID-19: social distancing, ACE 2 receptors, protease inhibitors and beyond? *Int J Clin Prac* **2020**, https://doi.org/10.1111/ijcp.13503.
4. Lippi, G.; Plebani, M. The critical role of laboratory medicine during coronavirus disease **2019,** (COVID-19) and other viral outbreaks. *Clin Chem Lab Med* **2020**, https://doi.org/10.1515/cclm-2020-0240.
5. Karako, K., Song, P., Chen, Y., Tang, W. Analysis of COVID-19 infection spread in Japan based on stochastic transition model. *BioSci Tre* **2020**. https://doi.org/10.5582/ bst. 2020. 014 82.
6. Wu, A.; Peng, Y.; Huang, B.; Ding, X.; Wang, X.; Niu, P.; Meng, J.; Zhu, Z.; Zhang, Z.; Wang, J.; Sheng, J.; Quan, L.; Xia, Z.; Tan, W.; Cheng, G.; Jiang, T. Genome Composition and Divergence of the Novel Coronavirus (2019-nCoV) Originating in China. *Cell Host & Microbe* **2020**, *27*, 325-328, https://doi.org/10.1016/j.chom.2020.02.001.
7. Cheepsattayakorn, A.; Cheepsattayakorn, R. Proximal origin and phylogenetic analysis of COVID-19 (2019-nCoV or SARS-CoV-2). *EC Microbiol* **2020**.
8. Guo, Y.R.; Cao, Q.D.; Hong, Z.S.; Tan, Y.Y.; Chen, S.D.; Jin, H.J.; Tan, K.S.; Wang, D.Y.; Yan, Y. The origin, transmission and clinical therapies on coronavirus disease 2019 (COVID-19) outbreak - an update on the status. *Mil Med Res* **2020**, *7*, https://doi.org/10.1186/s40779-020-00240-0.
9. Rothan, H.A.; Byrareddy S.N. The epidemiology and pathogenesis of coronavirus disease (COVID-19) outbreak. *J Autoimm* **2020**, *109*, https://doi.org/10.1016/j.jaut.2020.102433.
10. Koenig, K.L.; Beÿ, C.K.; McDonald, E.C. 2019-nCoV: the Identify-IsolateInform (3I) tool applied to a novel emerging coronavirus. *West J Emerg Med* **2020**, *21*, 184–90, https://dx.doi.org/10.5811%2Fwestjem.2020.1.46760.
11. Dany, L. COVID-19: protecting health-care workers. *Lancet* **2020**, *395*, https://doi.org/10.1016/S0140-6736(20)30644-9.
12. McCloskey, B.; Zumla, A.; Ippolito, G.; Blumberg, L.; Arbon, P.; Cicero, A.; Endericks, T.; Lim, P.L.; Borodina, M. Mass gathering events and reducing further global spread of COVID-19: a political and public health dilemma. *Lancet* **2020**, https://doi.org/10.1016/S0140-6736(20)30681-4.
13. Jin, Z.; Du, X.; Xu, Y.; Deng, Y.; Liu, M.; Zhao, Y.; Zhang, B.; Li, X.; Zhang, L.; Peng, C.; Duan, Y.; Yu, J.; Wang, L.; Yang, K.; Liu, F.; Jiang, R.; Yang, X.; You, T.; Liu, X.; Yang, X.; Bai, F.; Liu, H.; Liu, X.; Guddat, L.W.; Xu, W.; Xiao, G.; Qin, C.; Shi, Z.; Jiang, H.; Rao, Z.; Yang, H. Structure-based drug design, virtual screening and high-throughput screening rapidly identify antiviral leads targeting COVID-19. *BioRxiv* **2020,** https://doi.org/10.1101/2020.02.26.964882.
14. Wu, Y.; Guo, C.; Tang, L.; Hong, Z.; Zhou, J.; Dong, X.; Yin, H.; Xiao, Q.; Tang, Y.; Qu, X.; Kuang, L.; Fang, X.; Mishra, N.; Lu, J.; Shan, H.; Jiang, G.; Huang, X. Prolonged presence of SARS-CoV-2 viral RNA in faecal samples. *The Lancet Gastroenterology & Hepatology* **2020**, *5*, 434-435, https://doi.org/10.1016/S2468-1253(20)30083-2.
15. Mitjà, O.; Clotet, B. Use of antiviral drugs to reduce COVID-19 transmission. *Lancet Glob Health* **2020**, *8*, E638-E640, https://doi.org/10.1016/S2214-109X(20)30114-5.
16. Bashyam, A.M.; Feldman, S.R. Should patients stop their biologic treatment during the COVID-19 pandemic. *Journal of Dermatological Treatment* **2020**, *31*, 317-318, https://doi.org/10.1080/09546634.2020.1742438.
17. Mollaamin, F.; Monajjemi, M. DFT outlook of solvent effect on function of nano bioorganic drugs. *Physics and Chemistry of Liquids* **2012**, *50*, 596-604, https://doi.org/10.1080/00319104.2011.646444.
18. Mollaamin, F.; Gharibe, S.; Monajjemi, M. Synthesis of various nano and micro ZnSe morphologies by using hydrothermal method. *International Journal of Physical Sciences* **2011**, *6*, 1496-1500.
19. Monajjemi, M. Graphene/(h-BN)*n*/X-doped raphene as anode material in lithium ion batteries (X = Li, Be, B AND N,). *Macedonian Journal of Chemistry and Chemical Engineering* **2017**, *36*, 101–118, http://dx.doi.org/10.20450/mjcce.2017.1134.
20. Monajjemi, M. Cell membrane causes the lipid bilayers to behave as variable capacitors: A resonance with self-induction of helical proteins. *Biophysical Chemistry* **2015**, *207*, 114-127, https://doi.org/10.1016/j.bpc.2015.10.003.
21. Monajjemi, M. Study of CD5+ Ions and Deuterated Variants (CHxD(5-x)+): An Artefactual Rotation. *Russian Journal of Physical Chemistry A* **2018,** *92***,** 2215-2226.
22. Monajjemi, M. Liquid-phase exfoliation (LPE) of graphite towards graphene: An ab initio study. *Journal of Molecular Liquids*, **2017**, *230*, 461–472, https://doi.org/10.1016/j.molliq.2017.01.044.
23. Jalilian, H.; Monajjemi, M. Capacitor simulation including of X-doped graphene (X = Li, Be, B) as two electrodes and (h-BN)m (m = 1–4) as the insulator. *Japanese Journal of Applied Physics* **2015**, *54*, 085101-7.
24. Ardalan, T.; Ardalan, P.; Monajjemi, M. Nano theoretical study of a C 16 cluster as a novel material for vitamin C carrier. *Fullerenes Nanotubes and Carbon Nanostructures* **2014**, *22*, 687-708, https://doi.org/10.1080/1536383X.2012.717561.

25. Mahdavian, L.; Monajjemi, M.; Mangkorntong, N. Sensor response to alcohol and chemical mechanism of carbon nanotube gas sensors *Fullerenes Nanotubes and Carbon Nanostructures* **2009**, *17*, 484-495, https://doi.org/10.1080/15363830903130044.
26. Monajjemi, M.; Najafpour, J. Charge density discrepancy between NBO and QTAIM in single-wall armchair carbon nanotubes. *Fullerenes Nanotubes and Carbon Nano structures* **2014**, *22*, 575-594, https://doi.org/10.1080/1536383X.2012.702161.
27. Monajjemi, M.; Hosseini, M.S. Non bonded interaction of B16 N16 nano ring with copper cations in point of crystal fields. *Journal of Computational and Theoretical Nanoscience* **2013**, *10*, 2473-2477.
28. Monajjemi, M.; Mahdavian, L.; Mollaamin, F. Characterization of nanocrystalline silicon germanium film and nanotube in adsorption gas by Monte Carlo and Langevin dynamic simulation. *Bulletin of the Chemical Society of Ethiopia* **2008**, *22*, 277-286, https://doi.org/10.4314/bcse.v22i2.61299.
29. Lee, V.S.; Nimmanpipug, P.; Mollaamin, F.; Thanasanvorakun, S.; Monajjemi, M. Investigation of single wall carbon nanotubes electrical properties and normal mode analysis: Dielectric effects. *Russian Journal of Physical Chemistry A* **2009**, *83*, 2288-2296, https://doi.org/10.1134/S0036024409130184.
30. Mollaamin, F.; Najafpour, J.; Ghadami, S.; Akrami, M.S.; Monajjemi, M. The electromagnetic feature of B N H (x = 0, 4, 8, 12, 16, and 20) nano rings:Quantum theory of atoms in molecules/NMR approach. *Journal of Computational and Theoretical Nanoscience* **2014**, *11*, 1290-1298.
31. Monajjemi, M.; Mahdavian, L.; Mollaamin, F.; Honarparvar, B. Thermodynamic investigation of enolketo tautomerism for alcohol sensors based on carbon nanotubes as chemical sensors. *Fullerenes Nanotubes and Carbon Nanostructures* **2010**, *18*, 45-55, https://doi.org/10.1080/15363830903291564.
32. Monajjemi, M.; Ghiasi, R.; Seyed, S.M.A. Metal-stabilized rare tautomers: N4 metalated cytosine (M = Li, Na, K, Rb and Cs), theoretical views. *Applied Organometallic Chemistry* **2003**, *17*, 635-640, https://doi.org/10.1002/aoc.469.
33. Ilkhani, A.R.; Monajjemi, M. The pseudo Jahn-Teller effect of puckering in pentatomic unsaturated rings C AE , A=N, P, As, E=H, F, Cl.*Computational and Theoretical Chemistry* **2015**, *1074*, 19-25, http://dx.doi.org/10.1016%2Fj.comptc.2015.10.006.
34. Monajjemi, M. Non-covalent attraction of B N and repulsion of B N in the B N ring: a quantum rotatory due to an external field. *Theoretical Chemistry Accounts* **2015**, *134*, 1-22, https://doi.org/10.1007/s00214-015-1668-9.
35. Monajjemi, M.; Naderi, F.; Mollaamin, F.; Khaleghian, M. Drug design outlook by calculation of second virial coefficient as a nano study. *Journal of the Mexican Chemical Society* **2012**, *56*, 207-211, https://doi.org/10.29356/jmcs.v56i2.323.
36. Monajjemi, M.; Bagheri, S.; Moosavi, M.S. Symmetry breaking of B2N(-,0,+): An aspect of the electric potential and atomic charges. *Molecules* **2015**, *20*, 21636-21657, https://doi.org/10.3390/molecules201219769.
37. Monajjemi, M.; Mohammadian, N.T. S-NICS: An aromaticity criterion for nano molecules. *Journal of Computational and Theoretical Nanoscience* **2015**, *12*, 4895-4914, https://doi.org/10.1166/jctn.2015.4458.
38. Monajjemi, M.; Ketabi, S.; Hashemian, Z.M.; Amiri, A. Simulation of DNA bases in water: Comparison of the Monte Carlo algorithm with molecular mechanics force fields. *Biochemistry (Moscow)* **2006**, *71*, 1-8, https://doi.org/10.1134/s0006297906130013.
39. Monajjemi, M.; Lee, V.S.; Khaleghian, M.; Honarparvar, B.; Mollaamin, F. Theoretical Description of Electromagnetic Nonbonded Interactions of Radical, Cationic, and Anionic NH2BHNBHNH2 Inside of the B18N18 Nanoring. *J. Phys. Chem C* **2010**, *114*, 15315-15330, https://doi.org/10.1021/jp104274z.
40. Monajjemi, M.; Boggs, J.E. A New Generation of BnNn Rings as a Supplement to Boron Nitride Tubes and Cages. *J. Phys. Chem. A* **2013**, *117*, 1670-1684, https://doi.org/10.1021/jp312073q.
41. Monajjemi, M. Non bonded interaction between BnNn (stator) and BN B (rotor) systems: A quantum rotation in IR region. *Chemical Physics* **2013**, *425*, 29-45, https://doi.org/10.1016/j.chemphys.2013.07.014.
42. Monajjemi, M.; Robert, W.J.; Boggs, J.E. NMR contour maps as a new parameter of carboxyl's OH groups in amino acids recognition: A reason of tRNA–amino acid conjugation. *Chemical Physics* **2014**, *433*, 1-11, https://doi.org/10.1016/j.chemphys.2014.01.017.
43. Monajjemi, M. Quantum investigation of non-bonded interaction between the B15N15 ring and BH2NBH2 (radical, cation, and anion) systems: a nano molecularmotor. *Struct Chem* **2012,** *23*, 551–580, http://dx.doi.org/10.1007/s11224-011-9895-8.
44. Monajjemi, M. Metal-doped graphene layers composed with boron nitride–graphene as an insulator: a nanocapacitor. *Journal of Molecular Modeling* **2014**, *20*, https://doi.org/10.1007/s00894-014-2507-y.
45. Mollaamin, F.; Monajjemi, M.; Mehrzad, J. Molecular Modeling Investigation of an Anti-cancer Agent Joint to SWCNT Using Theoretical Methods. *Fullerenes, Nanotubes and Carbon Nanostructures* **2014**, *22*, 738-751, https://doi.org/10.1080/1536383X.2012.731582.
46. Monajjemi, M.; Ketabi, S.; Amiri, A. Monte Carlo simulation study of melittin: protein folding and temperature ependence. *Russian journal of physical chemistry* **2006**, *80*, S55-S62, https://doi.org/10.1134/S0036024406130103.

47. Monajjemi, M.; Heshmata, M.; Haeria, H.H. QM/MM model study on properties and structure of some antibiotics in gas phase: Comparison of energy and NMR chemical shift. *Biochemistry (Moscow)* **2006**, *71*, S113-S122, https://doi.org/10.1134/S0006297906130190.
48. Monajjemi, M.; Afsharnezhad, S.; Jaafari, M.R.; Abdolahi, T.; Nikosade, A.; Monajemi, H. NMR shielding and a thermodynamic study of the effect of environmental exposure to petrochemical solvent on DPPC, an important component of lung surfactant. *Russian Journal of Physical Chemistry A* **2007**, *81*, 1956-1963, https://doi.org/10.1134/S0036024407120096.
49. Mollaamin, F.; Noei, M.; Monajjemi, M.; Rasoolzadeh, R. Nano theoretical studies of fMET-tRNA structuren in protein synthesis of prokaryotes and its comparison with the structure of fALA-tRNA. *Africanjournal of microbiology research* **2011**, *5*, 2667-2674, https://doi.org/10.5897/AJMR11.310.
50. Monajjemi, M.; Heshmat, M.; Haeri, H.H.; Kaveh, F. Theoretical study of vitamin properties from combined QM-MM methods: Comparison of chemical shifts and energy. *Russian Journal of Physical Chemistry* **2006**, *80*, 1061-1068, https://doi.org/10.1134/S0036024406070119.
51. Monajjemi, M.; Chahkandi, B. Theoretical investigation of hydrogen bonding in Watson–Crick, Hoogestein and their reversed and other models: comparison and analysis for configurations of adenine–thymine base pairs in 9 models. *Journal of Molecular Structure: THEOCHEM* **2005**, *714*, 43-60, https://doi.org/10.1016/j.theochem.2004.09.048.
52. Monajjemi, M.; Honarparvar, B.; Haeri, H.H.; Heshmat, M. An ab initio quantum chemical investigation of solvent-induced effect on 14N-NQR parameters of alanine, glycine, valine, and serine using a polarizable continuum model. *Russian Journal of Physical Chemistry* **2006**, *80*, S40-S44, https://doi.org/10.1134/S0036024406130073.
53. Monajjemi, M.; Seyed Hosseini, M. Non Bonded Interaction of B16N16 Nano Ring with Copper Cations in Point of Crystal Fields. *Journal of Computational and Theoretical Nanoscience* **2013**, *10*, 2473-2477, https://doi.org/10.1166/jctn.2013.3233.
54. Monajjemi, M.; Farahani, N.; Mollaamin, F. Thermodynamic study of solvent effects on nanostructures: phosphatidylserine and phosphatidylinositol membranes. *Physics and Chemistry of Liquids* **2012**, *50*, 161-172, https://doi.org/10.1080/00319104.2010.527842.
55. Monajjemi, M.; Ahmadianarog, M. Carbon Nanotube as a Deliver for Sulforaphane in Broccoli Vegetable in Point of Nuclear Magnetic Resonance and Natural Bond Orbital Specifications. *Journal of Computational and Theoretical Nanoscience* **2014**, *11*, 1465-1471, https://doi.org/10.1166/jctn.2014.3519.
56. Monajjemi, M.; Ghiasi, R.; Ketabi, S.; Passdar, H.; Mollaamin, F. A Theoretical Study of Metal-Stabilised Rare Tautomers Stability: N4 Metalated Cytosine (M=Be2+, Mg2+, Ca2+, Sr2+ and Ba2+) in Gas Phase and Different. *Journal of Chemical Research* **2004**, *1*, 11-18, https://doi.org/10.3184/030823404323000648.
57. Monajjemi, M.; Baei, M.T.; Mollaamin, F. Quantum mechanic study of hydrogen chemisorptions on nanocluster vanadium surface. *Russian Journal of Inorganic Chemistry* **2008**, *53*, 1430-1437, https://doi.org/10.1134/S0036023608090143.
58. Mollaamin, F.; Baei, M.T.; Monajjemi, M.; Zhiani, R.; Honarparvar, B. A DFT study of hydrogen chemisorption on V (100) surfaces. *Russian Journal of Physical Chemistry A, Focus on Chemistry* **2008**, *82*, 2354-2361, https://doi.org/10.1134/S0036024408130323.
59. Monajjemi, M.; Honarparvar, B.; Nasseri, S.M.; Khaleghian, M. NQR and NMR study of hydrogen bonding interactions in anhydrous and monohydrated guanine cluster model: A computational study. *Journal of Structural Chemistry* **2009**, *50*, 67-77, https://doi.org/10.1007/s10947-009-0009-z.
60. 55. Monajjemi, M.; Aghaie, H.; Naderi, F. Thermodynamic study of interaction of TSPP, CoTsPc, and FeTsPc with calf thymus DNA. *Biochemistry (Moscow)* **2007**, *72*, 652-657, https://doi.org/10.1134/S0006297907060089.
61. Monajjemi, M.; Heshmat, M.; Aghaei, H.; Ahmadi, R.; Zare, K. Solvent effect on 14N NMR shielding of glycine, serine, leucine, and threonine: Comparison between chemical shifts and energy versus dielectric constant. *Bulletin of the Chemical Society of Ethiopia* **2007**, *21*, 111-116, https://doi.org/10.4314/bcse.v21i1.61387.
62. Monajjemi, M.; Rajaeian, E.; Mollaamin, F.; Naderi, F.; Saki, S. Investigation of NMR shielding tensors in 1,3 dipolar cycloadditions: solvents dielectric effect. *Physics and Chemistry of Liquids* **2008**, *46*, 299-306, https://doi.org/10.1080/00319100601124369.
63. Mollaamin, F.; Varmaghani, Z.; Monajjemi, M. Dielectric effect on thermodynamic properties in vinblastine by DFT/Onsager modelling. *Physics and Chemistry of Liquids* **2011**, *49*, 318-336, https://doi.org/10.1080/00319100903456121.
64. Monajjemi, M.; Honaparvar, B.; Khalili Hadad, B.; Ilkhani, A.; Mollaamin, F. Thermo-Chemical Investigation and NBO Analysis of Some anxileotic as Nano- Drugs. *African journal of pharmacy and pharmacology* **2010**, *4*, 521-529.
65. Monajjemi, M.; Khaleghian, M.; Mollaamin, F. Theoretical study of the intermolecular potential energy and second virial coefficient in the mixtures of CH4 and Kr gases: a comparison with experimental data. *Molecular Simulation* **2010**, *36*, 865-870, https://doi.org/10.1080/08927022.2010.489557.

66. Monajjemi, M.; Khosravi, M.; Honarparvar, B.; Mollaamin, F. Substituent and solvent effects on the structural bioactivity and anticancer characteristic of catechin as a bioactive constituent of green tea. *International Journal of Quantum Chemistry* **2011**, *111*, 2771-2777, https://doi.org/10.1002/qua.22612.
67. Tahan, A.; Monajjemi, M. Solvent dielectric effect and side chain mutation on the structural stability of Burkholderia cepacia lipase active site: a quantum mechanical/molecular mechanics study. *Acta Biotheor* **2011**, *59*, 291-312, https://doi.org/10.1007/s10441-011-9137-x.
68. Monajjemi, M.; Khaleghian, M. EPR Study of Electronic Structure of [CoF6]3-and B18N18 Nano Ring Field Effects on Octahedral Complex. *Journal of Cluster Science* **2011**, *22*, 673-692, https://doi.org/10.1007/s10876-011-0414-2.
69. Monajjemi, M.; Mollaamin, F. Molecular Modeling Study of Drug-DNA Combined to Single Walled Carbon Nanotube. *Journal of Cluster Science* **2012**, *23*, 259-272, https://doi.org/10.1007/s10876-011-0426-y.
70. Mollaamin, F.; Monajjemi, M. Fractal Dimension on Carbon Nanotube-Polymer Composite Materials Using Percolation Theory. *Journal of Computational and Theoretical Nanoscience* **2012**, *9*, 597-601, https://doi.org/10.1166/jctn.2012.2067.
71. Mahdavian, L.; Monajjemi, M. Alcohol sensors based on SWNT as chemical sensors: Monte Carlo and Langevin dynamics simulation. *Microelectronics Journal* **2010**, *41*, 142-149, https://doi.org/10.1016/j.mejo.2010.01.011.
72. Monajjemi, M.; Falahati, M.; Mollaamin, F. Computational investigation on alcohol nanosensors in combination with carbon nanotube: a Monte Carlo and ab initio simulation. *Ionics* **2013**, *19*, 155-164, https://doi.org/10.1007/s11581-012-0708-x.
73. Ghalandari, B.; Monajjemi, M.; Mollaamin, F.; Theoretical investigation of carbon nanotube Binding to DNA in View of Drug Delivery. Journal of Computational and Theoretical Nanoscience , **2011**, 8 (7), 1212-1219.
74. Monajjemi, M., Mahdavian, L.; Mollaamin, F.; Khaleghian, M.; Interaction of Na, Mg, Al, Si with carbon nanotube (CNT): NMR and IR study.,Russian Journal of Inorganic Chemistry 54 (9),1465 1473.
75. Mollaamin, F.; Monajjemi, M, Harmonic Linear Combination and Normal Mode Analysis of Semiconductor Nanotubes Vibrations., Journal of Computational and Theoretical Nanoscience, **2015**, *12 (6)*, 1030-1039.
76. Cui, J.; Shi, Z.L. Origin and evolution of pathogenic coronaviruses. *Nat. Rev. Microbiol.* **2019**, *17*, 181-192, https://doi.org/10.1038/s41579-018-0118-9.
77. Park, Y.J.; Walls, A.C.; Wang, Z.; Sauer, M.; Li, W.; Tortorici, M.A.; Bosch, B.J.; DiMaio, F.D.; Veesler, D. Seattle Structural Genomics Center for Infectious Disease (SSGCID). *Nat. Struct. Mol. Biol.* **2019,** *26*, 1151-1157, https://doi.org/10.1038/s41594-019-0334-7.